Pulsed Neutron Source Reference Measurements in the Subcritical Experiment YALINA-Booster

C. Berglöf [1], M. Fernández-Ordóñez [2], D. Villamarín [2], V. Bécares [2], E. M. González-Romero [2], V. Bournos [3], I. Serafimovich [3], S. Mazanik [3], Y. Fokov [3], H. Kiyavitskaya [3]

[1] Royal Institute of Technology (KTH), Department of Reactor Physics, Stockholm, Sweden
[2] CIEMAT, Nuclear Innovation Group, Avda. Complutense, Madrid, Spain
[3] Joint Institute for Power and Nuclear Research, Nat. Academy of Sciences, Minsk, Belarus

Email contact of main author: calle@neutron.kth.se

Abstract. In support of an online reactivity monitoring experiment, also presented in this conference, this work presents the reactivity calibration measurements performed with a pulsed neutron source in the coupled fast-thermal subcritical facility YALINA-Booster. These experiments reveal the complexity of experimentally obtaining a global reactivity from a highly heterogeneous core. Moreover, the effect of varying the source multiplication at constant reactivity on the area ratio technique is explored. It is found that the reactivity obtained with the area ratio technique carry strong spatial dependence, but it can be handled by calculated correction factors. On the other hand the method is showed not to be sensitive to changes in the source multiplication. It is also shown that the prompt neutron decay constant does not vary strongly over the core except at deep subcritical states.

1. Introduction

An extensive experimental program devoted to reactivity monitoring of accelerator-driven systems has been carried out at the zero-power subcritical facility YALINA-Booster. This work is a part of a joint collaboration between several European research institutes through the European research programme for the transmutation of high level nuclear waste in an accelerator-driven system (IP-EUROTRANS) in the 6th EU Framework Programme. One of the main objectives of the IP-EUROTRANS experiments at the YALINA-Booster facility is to validate and test a possible online reactivity monitoring technique[1-3]. For this purpose, a set of reactivity determination measurements was performed to obtain reference reactivity values for the configurations studied. The methods applied are the area ratio technique by Sjöstrand[4] and the prompt neutron decay fitting technique[5,6].
Besides obtaining reference reactivity values, the scope of the experiments has been to investigate the performance of the reactivity determination techniques in a broad range of subcriticalities and for different source multiplications. The latter was obtained by substituting highly enriched fuel in the centre of the core (close to the neutron source) by low enriched fuel at the core periphery. In this way the effective multiplication factor (k_{eff}) could be kept constant while altering the source multiplication (k_s). This was done at $k_{eff} \sim 0.95$. In addition, two configurations at subcriticality levels 0.977 and 0.85 were investigated.

2. Experimental Setup

The YALINA-Booster is a subcritical fast-thermal core coupled to a neutron generator[7]. The neutron generator uses a deuteron ion accelerator impinging on a, in these experiments, Ti-T target to produce 14 MeV neutrons. The deuteron accelerator can be operated in both continuous and pulse modes and gives thereby the possibility to perform both pulsed neutron source (PNS) measurements and continuous wave measurements. The maximum beam current in continuous mode is around 1.5 mA giving a maximum neutron yield of approximately 10^{11} neutrons per second.

The core, depicted in FIG. 1, consists of a central lead zone (booster), a polyethylene zone, a radial graphite reflector and a front and back biological shielding of borated polyethylene. The fast-spectrum lead zone and the thermal-spectrum polyethylene zone are separated by a so called thermal neutron filter, or valve zone, consisting of one layer of 108 pins with metallic natural uranium and one layer of 116 pins with boron carbide (B_4C), which are located in the outermost two rows of the fast zone. Hence, thermal neutrons diffusing from the thermal zone to the fast zone will either be absorbed by the boron or by the natural uranium. In this way, a coupling of mainly fast neutrons between the two zones is maintained. The different experimental channels (EC or MC) used in these experiments are indicated in FIG. 1.

The three B_4C-control rods that can be inserted in the thermal zone allow to change the reactivity of the system by about 0.5$. Hence, the sensitivity of the different reactivity monitoring techniques can be tested.

Four different loadings, described in TABLE I, were investigated. The aim when choosing the different loadings was to have one configuration as near critical as possible (taking into account regulation restrictions), two configurations with similar k_{eff} but different k_s and one deep subcritical configuration. The fuel in the innermost part of the booster zone could be uranium oxide of 36% enrichment or metallic uranium of 90% enrichment, whereas the rest of the fast booster zone consisted of 36% enriched uranium oxide fuel. The thermal zone was loaded with uranium oxide of 10% enrichment. All configurations, except SC6 were studied with the control rods both inserted and withdrawn, thus giving in total seven configurations.

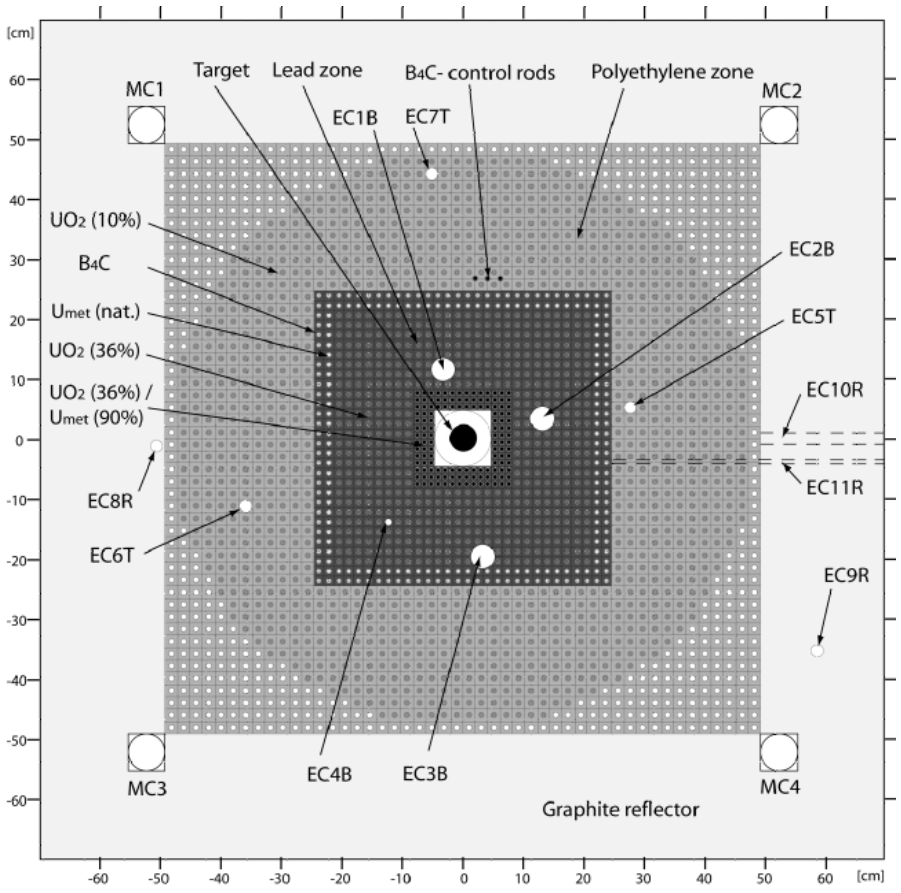

FIG. 1. Schematic cross-sectional view of the YALINA-Booster reactor core (SC0).

TABLE I: CORE CONFIGURATIONS.

Zone:	Inner booster		Outer booster	Thermal zone	Expected*
Enr:	90%	36%	36%	10%	k_{eff}
SC0	132	-	563	1141	0.977
SC3a	-	132	563	1077	0.950
SC3b	-	-	563	1090	0.950
SC6	-	132	563	726	0.850

* Based on MCNP[8] calculations.

3. Experimental Results

3.1. Reactivity Determination

By operating the neutron generator in pulse mode and registering the detector signals after each pulse, histograms of pulses were produced by adding data from all pulses to each other. From such PNS histograms the reactivity of the system can be found in two ways. Firstly, the reactivity can be found from the prompt neutron decay constant[5,6]:

$$\alpha = \frac{\rho - \beta_{eff}}{\Lambda}. \tag{1}$$

In Eq. (1), all symbols follow those usually used in reactor physics literature. Secondly, the reactivity can be obtained from the ratio of the areas under the pulse described by the flux caused by prompt neutrons only (A_p) and the flux caused by delayed neutrons only (A_d)[4]:

$$\rho_{\$} \equiv \frac{\rho}{\beta_{eff}} = -\frac{A_p}{A_d}. \tag{2}$$

3.2. Experimental Results

Some characteristic PNS histograms acquired by fission chambers of 500 mg and 1 mg ^{235}U deposit are shown in FIG. 2. The most interesting behavior can be found in the data from the fission chamber located in the booster region (EC2B). A very fast flux decay can be found within a few microseconds after the source pulse. During this time, the flux decreases about two orders of magnitude. Then, in all detectors, a prompt neutron decay follows for about 7 ms (SC3a). During this decay, the flux is, in the entire core, driven by the fundamental mode of the thermal region. This means that despite the complex heterogeneity of the core, there seems to exist a global prompt neutron decay constant. This is true for the booster zone and the thermal zone, however, the decay constant as measured in the reflector (MC2) is slightly lower than in the rest of the core. This effect becomes more pronounced at deep subcriticality as can be seen in FIG. 2 for configuration SC6. Fitted values for α as well as reactivity values from the area ratio method ($\rho_{\$}$) can be found in TABLE II.

The most important observation from these measurements is the large deviation in area ratio reactivity as obtained from the detectors in the booster region. As can be seen in TABLE II, the reactivity when measured in the booster region can be up to a factor of two larger than the corresponding measurement in the thermal region. The explanation to the large deviation comes from the large prompt area caused by the peak during and shortly after the neutron pulse. A zoom of PNS histograms in the booster zone during the first 30 μs after pulse insertion is given in FIG. 3. In the same figure, the shape of the source is given in blue.

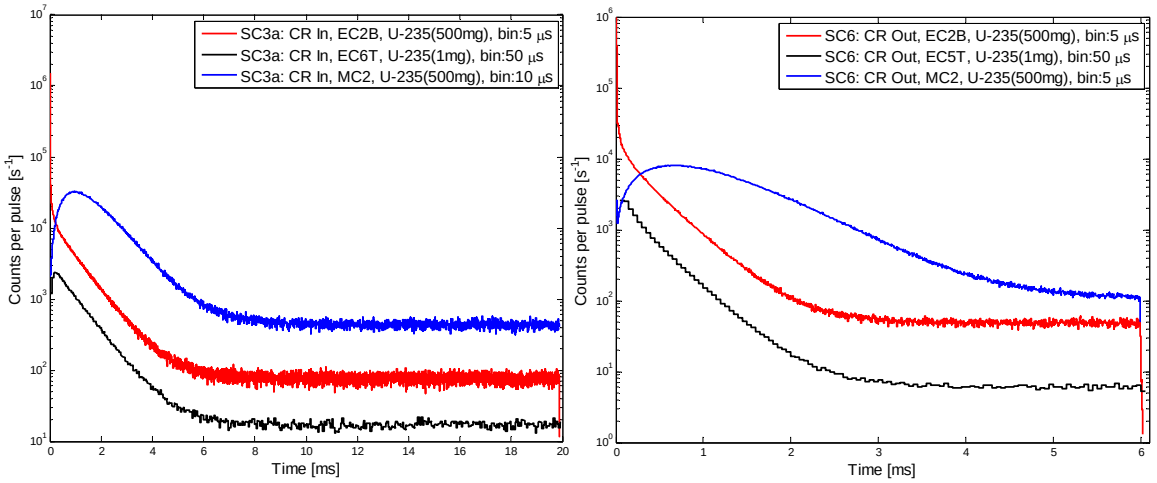

FIG. 2. PNS histograms for the configurations SC3a (control rods inserted) and SC6 (control rods withdrawn).

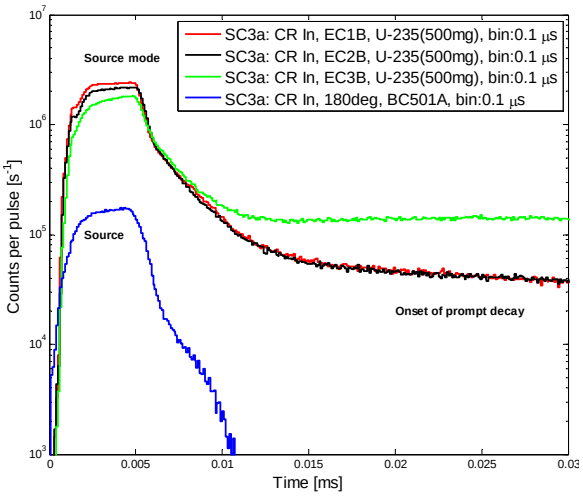

FIG. 3. PNS histograms for conf. SC3a and detectors in the booster zone during the first 30 μs after pulse insertion.

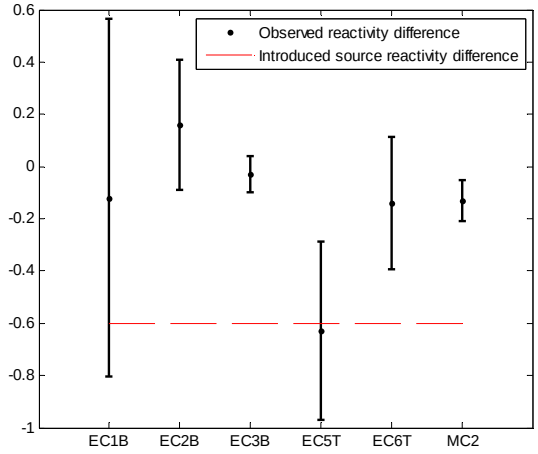

FIG. 4. Area method reactivity differences between SC3b and SC3a. The magnitude of the source reactivity change is indicated with a dashed line.

3.3. Source Multiplication Effects

The layout of configurations SC3a and SC3b was iterated be means of MCNP calculations to give the same value of k_{eff} with as large perturbation of the inner booster zone as possible. The source multiplication, defined as

$$k_s = \frac{M}{M+S}. \tag{3}$$

where M is the total neutron source in the system and S is the external source strength[9], was also estimated by MCNP calculations. It was found that the difference in k_s between SC3a and SC3b is approximately 500 pcm (~0.6$). The purpose of the measurements on SC3a and SC3b was to identify a possible influence from k_s on the area ratio technique. In FIG. 4, the difference in reactivity between SC3b and SC3a are shown. When comparing, one must keep in mind that it is assumed that a possible difference in effective delayed neutron fraction between the two configurations is negligible. As can be seen, the area ratio reactivity is comparable in all channels. Consequently, the area ratio method preserves the reactivity value when changing the source reactivity (indicated by dashed line).

TABLE II: EXPERIMENTAL RESULTS.

		α [s^{-1}]		$\rho_{\$}$ [\$]	
		CR Out	CR In	CR Out	CR In
SC0	EC1B	-636±1	-699±2	-	-
	EC2B	-639±1	-	-	-
	MC2	-612±1	-	-3.51±0.01	-
SC3a	EC1B	-1051.4±1.6	-1117.1±2.2	-14.89±0.20	-17.12±0.27
	EC2B	-	-1112.0±1.9	-	-15.27±0.17
	EC3B	-	-1096.7±1.0	-	-10.13±0.05
	EC5T	-1053.4±9.3	-1081±15	-8.68±0.34	-9.42±0.21
	EC6T	-	-1090.9±2.9	-	-7.46±0.14
	MC2	-984.9±5.4	-1031.7±7.6	-7.21±0.03	-7.83±0.06
	MC3	-944±19	-1009±27	-7.23±0.94	-7.86±1.11
SC3b	EC1B	-1034.9±3.7	-1113.0±3.8	-14.97±0.47	-17.24±0.63
	EC2B	-1041.1±1.7	-1099.5±2.0	-13.77±0.16	-15.11±0.18
	EC3B	-1035.7±0.9	-1086.5±1.3	-9.59±0.04	-10.16±0.05
	EC5T	-1042.9±4.5	-1095.0±6.6	-9.24±0.23	-10.05±0.27
	EC6T	-1026.2±3.7	-1088.0±4.7	-7.40±0.20	-7.60±0.21
	MC2	-969.8±2.9	-1010.1±2.7	-7.29±0.04	-7.96±0.05
SC6	EC2B	-2607±5.6	-	-41.93±0.67	-
	EC5T	-2614±13	-	-23.49±0.85	-
	MC2	-1568±29	-	-20.12±0.18	-

4. Two-Region Point Kinetic Model

The simplest way to describe the deviating results obtained by the area ratio method in the fast booster zone is to extend the point kinetic equations to two regions. By treating the flux caused by delayed neutrons separately, the solution to the area reactivity, Eq. (2), can be obtained. A two-region point kinetic model with prompt and delayed neutron fluxes can be expressed as follows:

$$\begin{cases} \dfrac{dn_{p1}(t)}{dt} = \alpha_1 n_{p1}(t) + \dfrac{f_{21}}{\tau_2} n_{p2}(t) + S(t) \\ \dfrac{dn_{d1}(t)}{dt} = \alpha_1 n_{d1}(t) + \dfrac{f_{21}}{\tau_2} n_{d2}(t) + \lambda C_1(t) \\ \dfrac{dC_1(t)}{dt} = \dfrac{\beta_1}{\Lambda_1}\left(n_{p1}(t) + n_{d1}(t)\right) - \lambda C_1(t) \\ \dfrac{dn_{p2}(t)}{dt} = \alpha_2 n_{p2}(t) + \dfrac{f_{12}}{\tau_1} n_{p1}(t) \\ \dfrac{dn_{d2}(t)}{dt} = \alpha_2 n_{d2}(t) + \dfrac{f_{12}}{\tau_1} n_{d1}(t) + \lambda C_2(t) \\ \dfrac{dC_2(t)}{dt} = \dfrac{\beta_2}{\Lambda_2}\left(n_{p2}(t) + n_{d2}(t)\right) - \lambda C_2(t) \end{cases} \quad (4)$$

In these equations n_{pi} is the prompt neutron flux density in region i, n_{di} is the delayed neutron flux density in region i, C_i is the delayed neutron precursor density in region i, α_i is the prompt neutron decay constant in region i, f_{ij} is the probability that a neutron escapes from region i to region j, τ_i is the neutron lifetime in region i, S is the external source strength, β_i is the effective delayed neutron fraction in region i, Λ_i is the mean neutron generation time (reproduction time) in region i and λ is the one delayed neutron group decay constant. In the

case of YALINA-Booster, region 1 is the booster region, where the source is located, and region 2 is the thermal zone.
The neutron flux areas of Eq. (2) are obtained by integrating the neutron fluxes from zero to infinity. If assuming a Dirac source pulse, the left hand side of Eq. (4) will be zero:

$$\begin{cases} 0 = \alpha_1 A_{p1} + \dfrac{f_{21}}{\tau_2} A_{p2} + S_0 \\ 0 = \alpha_1 A_{d1} + \dfrac{f_{21}}{\tau_2} A_{d2} + \dfrac{\beta_1}{\Lambda_1}\left(A_{p1} + A_{d1}\right) \\ 0 = \alpha_2 A_{p2} + \dfrac{f_{12}}{\tau_1} A_{p1} \\ 0 = \alpha_2 A_{d2} + \dfrac{f_{12}}{\tau_1} A_{d1} + \dfrac{\beta_2}{\Lambda_2}\left(A_{p2} + A_{d2}\right) \end{cases} \tag{5}$$

An expression for the area ratio reactivity in each region can be derived by solving for the prompt and delayed areas in the two regions: A_{p1}, A_{d1}, A_{p2} and A_{d2}. By assuming

$$|\alpha_1| \gg |\alpha_2|, \tag{6}$$

which is the case in YALINA-Booster, the area ratio reactivities can be expressed as

$$\rho_{\$1} = -\frac{A_{p1}}{A_{d1}} \approx \frac{\rho_2}{\beta_2}\left(\frac{1}{f}\alpha_1\tau_1\alpha_2\tau_2 - 1\right) - 1, \tag{7}$$

$$\rho_{\$2} = -\frac{A_{p2}}{A_{d2}} \approx \frac{\rho_2}{\beta_2}\left(1 - f\frac{1}{\alpha_1\tau_1}\right) - f\frac{1}{\alpha_1\tau_1\beta_2}, \tag{8}$$

where ρ_i is the local reactivity in region i (obeying Eq. (1)) and f is the return probability given by the product $f_{12}f_{21}$.
In both regions the area ratio reactivity is based on the local reactivity in the thermal region with a factor and a term describing the coupling effect with the booster region. One should notice that, in the booster region, the return probability appear in the denominator, thus affecting the result stronger than in the thermal region where the return probability appear in the nominator. Numerically, it can easily be verified that $\rho_{\$2}$ is the best estimate of the combined global reactivity of the subsystems 1 and 2. The combined global effective multiplication constant, k, is given by

$$k = \frac{k_1 + k_2}{2} + \sqrt{\left(\frac{k_1 + k_2}{2}\right)^2 + f}, \tag{9}$$

where k with sub-index is the effective multiplication constant of each region respectively[10]. Consequently, the reactivity value obtained in the booster region, $\rho_{\$1}$, is the biased result.

5. Spatial Correction Factors

In the previous section, a two-region kinetic model has been presented to explain the deviations observed in the reactivity estimation provided by the Sjöstrand area ratio method at different detector positions. Even more, it has been shown that, in general, even taking detectors where the dispersion is small, the area method returns a biased estimation of the reactivity. Hence, it is necessary to obtain a correction factor which takes into account the complete description of the system. This correction factor can be obtained from MCNP[8] calculations (other simulation tools can be used to investigate spatial and energy effects for the area method as shown by. M. Carta. et al.[11]).

Let us start by rewriting Eq. (2) in the form:

$$\rho_{\$} \equiv \frac{\rho}{\beta_{eff}} = -\frac{A_p}{A_d} = \left(1 - \frac{A_t}{A_p}\right)^{-1}, \tag{10}$$

where A_t denotes the area due both to prompt and delayed neutrons, that is, $A_t = A_p + A_d$. A_p and A_t can be calculated for every detector location with MCNP just enabling or disabling the delayed neutron transport. In this way, MCNP can provide an estimator of the area method reactivity, $\rho_{\text{MCNP, detector}}$, for any detector position.
On the other hand, a criticality calculation can also be performed with MCNP to obtain a value for the effective multiplication constant and the effective delayed neutron fraction of the system, which allow us to calculate the global reactivity, ρ_{MCNP}. Thus, a correction factor for the area method in every detector location can be obtained in the following way:

$$C_{\text{detector}} = \frac{\rho_{\text{MCNP, detector}}}{\rho_{MCNP}}. \tag{11}$$

Once these correction factors have been obtained, the reactivity of the system can be estimated in a straightforward way, just replacing in the last equation the reactivity estimates by MCNP for every location by the experimental ones:

$$\rho = \frac{\rho_{\text{experimental, detector}}}{C_{\text{detector}}}. \tag{12}$$

The correction factors have been computed using the JEFF3.1 nuclear data library and the reactivity values thus obtained are listed in TABLE III. It must be pointed out that the observed uncertainty in the determination of the correction factors decreases much slower than the statistical uncertainty, hence, to obtain a good estimation, it is necessary to run each case for the equivalent of 800 cpu-days.
By inspecting TABLE III it can be observed that the dispersion of the data is greatly reduced, and most of the detectors are compatible among themselves. Furthermore, the reactivity values obtained for the SC3a and SC3b configurations are close, as it was expected according to MCNP simulations.

6. Conclusions

A set of pulsed neutron source measurements have been performed in the subcritical assembly YALINA-Booster. The reactivity values obtained carry a strong spatial dependence as an effect of the heterogeneity of the core. On the other hand, it was found that the prompt neutron decay was comparable in all detectors except for the detector in the reflector at deep subcriticality. When altering the source multiplication at constant reactivity, the area ratio method still gave the same reactivity value. The strong spatial spread of the area ratio method could be handled by applying correction factors obtained through Monte Carlo simulations.

TABLE III: CORRECTION FACTORS AND CORRECTED REACTIVITY FOR SC3A AND SC3B.

	SC3a			SC3b		
	$C_{detector}$	$\rho_{corrected}$ [$]			$\rho_{corrected}$ [$]	
		CR out	CR in	$C_{detector}$	CR out	CR in
EC1B	1.81 ± 0.03	-8.21 ± 0.16	-9.44 ± 0.20	1.94 ± 0.03	-7.71 ± 0.28	-8.87 ± 0.36
EC2B	1.63 ± 0.02	---	-9.39 ± 0.17	1.73 ± 0.03	-7.98 ± 0.16	-8.76 ± 0.18
EC3B	1.10 ± 0.02	---	-9.21 ± 0.15	1.12 ± 0.02	-8.56 ± 0.14	-9.07 ± 0.15
EC5T	0.98 ± 0.02	-8.86 ± 0.38	-9.62 ± 0.27	1.00 ± 0.02	-9.23 ± 0.28	-10.04 ± 0.32
EC6T	0.85 ± 0.01	---	-8.78 ± 0.22	0.85 ± 0.01	-8.70 ± 0.27	-8.93 ± 0.29
MC2	0.85 ± 0.01	-8.45 ± 0.14	-9.17 ± 0.16	0.85 ± 0.01	-8.56 ± 0.15	-9.34 ± 0.16
MC3	0.83 ± 0.01	-8.66 ± 1.13	-9.42 ± 1.34	0.86 ± 0.01	---	---
Weighted average		-8.39 ± 0.10	-9.24 ± 0.08		-8.42 ± 0.08	-9.11 ± 0.08

Acknowledgements

This work was supported by IP-EUROTRANS contract FI6W-CT2005-516520, the ENRESA-CIEMAT agreement for the *Transmutación Aplicada a los Residuos Radiactivos de Alta Actividad* and the Swedish Institute through the *Visby program*.

References

1. VILLAMARÍN , D. et al, "Current-to-flux and reactivity monitoring of a subcritical assembly using beam trips and current mode detectors: The YALINA-Booster program", *This conference*.
2. BÉCARES, V. et al, "Reactivity Monitoring with Imposed Beam Trips and Pulsed Mode Detectors in the Subcritical Experiment YALINA-Booster", *This conference*.
3. BERGLÖF, C. et al, "Neutron Noise Measurements in the YALINA-Booster Experiments", *This conference*.
4. SJÖSTRAND, N. G., "Measurement on a subcritical reactor using a pulsed neutron source", *Arkiv för fysik,* 11, 13 (1956).
5. MASTERS, C. F. and CADY, K. B., "A procedure for evaluating modified pulsed-neutron source experiments in subcritical nuclear reactors". Nuclear Science and Engineering, 29 (1967).
6. SIMMONS, B. E. and KING J. S., "A Pulsed Technique for Reactivity Determination", Nuclear Science and Engineering, 3, 595-608 (1958).
7. CHIGRINOV, S. E. et al., "Booster Subcritical Assembly Driven by a Neutron Generator", Preprint JIPNR-Sosny, Minsk, p. 31 (2004). (In Russian).
8. X-5 MONTE CARLO TEAM, "MCNP – A General Monte Carlo N-Particle Transport Code, Version 5", LA-UR-03-1987, Los Alamos National Laboratory, USA (2005).
9. SALVATORES, M. et al., "The Potential of Accelerator-Driven Systems for Transmutation or Power Production Using Thorium or Uranium Fuel Cycles", Nuclear Science and Engineering, 126, 333 (1997).
10. AVERY, R. , "Theory of Coupled Reactors", Proc. of the Second United Nations International Conference on the Peaceful Uses of Atomic Energy, Vol. 12, pp. 182-191, United Nations, Geneva, Switzerland (1958).
11. CARTA, M. et al. "Reactivity assessment and spatial time-effects from the MUSE kinetics experiments". Proc. of PHYSOR 2004 - The Physics of Fuel Cycles and Advanced Nuclear Systems: Global Developments, Chicago, Illinois, USA, April 25-29 (2004).